

## **Justification of parameters of seed treater with an eccentrically fixed drum influencing the motion character and seed treatment modes**

**Eduard Khasanov, Ildar Gabitov, Salavat Mudarisov, Rim Khamaletdinov, Zinnur Rakhimov, Ilshat Akhmetyanov, Ildar Farkhutdinov\*, Ilgam Masalimov, Radik Musin**

*Federal State Budgetary Educational Establishment of Higher Education “Bashkir State Agrarian University”, Ufa 450001, Bashkortostan, Russia*

*\*Corresponding author: hasan\_ed@mail.ru*

### **Abstract**

Khasanov, E., Gabitov, I., Mudarisov, S., Khamaletdinov, R., Rakhimov, Z., Akhmetyanov, I., Farkhutdinov, I., Masalimov, I., & Musin, R. (2019). Justification of parameters of seed treater with an eccentrically fixed drum influencing the motion character and seed treatment modes. *Bulgarian Journal of Agricultural Science, 25 (Suppl. 2)*, 119–128

The examination of the state of the problem shows that the lack of serial treating machines capable of high-quality, high-coverage treatment with microbiological preparations prevents the widespread practice of treating seeds with biological products. Among the machines produced, the most suitable for using microbiological preparations are drum-type treaters, in which the distribution of a biological product is carried out using a nozzle, which does not have a detrimental effect on microorganisms. However, the quality of their work, assessed by the coefficient of seed surface coverage with the preparation, does not exceed 70%, which does not meet agro-technical requirements. In this regard, the aim of the work is to improve the quality of seed coverage with a biological preparation with a drum-type treater by improving and substantiating its structural and technological parameters. It was established that in order to improve the quality of the treatment process with drum treaters, a non-stationary mode of moving seeds inside the working drum is necessary. This is realized by eccentric fastening of the drum, which ensures the non-stationary mode of moving seeds relative to the working surface during its operation. As a result, its working surface is most fully used and, as a result, the quality of the seed treatment process is improved. The technique is considered and a mathematical model of seed movement in a drum treatment machine for pre-sowing treatment is proposed, which provides an increase in the quality of the coating. The studies of the seed movement inside an eccentrically fixed drum are carried out. The paper deals with dependences that determine the conditions of relative dormancy and detachment of the seed from the inner surface of the drum. The proposed mathematical model of the movement of a seed inside an eccentrically fixed drum of a seed treater allows its structural and technological parameters to be determined during non-stationary operation.

**Keywords:** plant science; drum treatment; machine; pre-sowing treatment; seed movement; non-stationary mode; coating quality

### **Introduction**

One of the main conditions for obtaining high yields of grain crops is the use of high-quality seeds (Hozzein et al., 2019). In the complex of measures ensuring the obtaining of seeds of good quality, the correct implementation of mea-

asures to combat fungal, bacterial and virus diseases of plants, and especially those of them that are transmitted through seed material, is important (Khamaletdinov et al., 2009a; Li et al., 2018). Diseases of cereals propagating through seeds impair their sowing qualities and cause a significant decrease in yield. In addition, infected seeds are a source for the further

spread of plants diseases (Kadege & Lyimo, 2015; Lopez-Reyes et al., 2016; Zegeye et al., 2017).

Currently, the main method of protecting seeds from pests and diseases is the use of chemicals (treatment). It allows reducing potential yield losses by 50-55% (Cessna & Westcott, 2018), which determines its primary use in plant protection systems, in addition, seed treatment is a more cost-effective way to control diseases than spraying crops (Najar et al., 2017).

However, in most developed countries of the world, scientists have come to the unequivocal conclusion (Nasu et al., 2018). This is due to the fact that all chemical preparations, as well as dust emissions during their seed treatment, cause chronic poisoning of soil, water and air (Zaller et al., 2016; Rudelt et al., 2017), and the accumulated residues in agricultural food and feed reduce their biological value and safety (Annis, 2016).

Currently, technologies have been developed for the production and use of biological products based on symbiotic and associative nitrogen-fixing and phosphate-mobilizing microorganisms, as well as microorganisms producing phytohormones, vitamins, organic acids, antibiotics and other biologically active substances (Gurav et al., 2017).

This helps to improve the mineral nutrition of plants, increase their resistance to various stresses and phytopathogens, increase yields and quality of crop production while preserving and fertility of the soil (Ivantsova et al., 2015; Kosulnikov & Laktionov, 2018; Moharam et al., 2018; Oral et al., 2018). But the widespread use of biological products in the practice of agriculture is hampered by the fact that there are no technical means for seed treatment of grain crops adapted for using microbiological preparations, which in turn significantly reduces their effectiveness (Kamaletdinov et al., 2007). We have investigated the influence of technological processes occurring in technical means for treatment on the vital activity of bacteria of the genus *Bacillus subtilis*. According to them, when using devices that distribute a biological product using discs, the microorganisms used are significantly inhibited, while the effect of overpressure, spraying through a nozzle, and seed treatment in the drum did not affect the development of colonies of microorganisms (Kamaletdinov et al., 2007).

In addition, our research on injuring seeds during their pre-sowing treatment showed that their least damage occurs when using drum treaters ((Kamaletdinov et al., 2009a), the disadvantage of which is the stationary mode of seed movement that does not allow full use of the working volume of the treater chamber (Figure 1a) (Reznichenko, 1964).

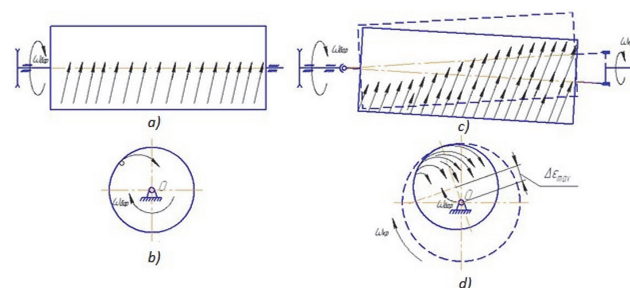


**Fig. 1. Using the working volume of the drum:**  
**a – traditional drive method (top view); b – the proposed drive method (top view); c, d – the cross section of the drum with the traditional and the proposed methods of drives**

The long-term experimental studies have established that eccentric fixing of the drum of the treater with the correct choice of the kinematic mode provides a non-stationary mode of moving the seeds (Figure 1c). Based on the obtained results, we developed a device for pre-sowing treatment of seeds, which was confirmed by a patent for a useful model (Kamaletdinov et al., 2009b).

On this basis, it is advisable to use drum-type treaters, in which the distribution of the biological product is carried out using a nozzle. An urgent task is the modernization of the drum treater with the introduction of new structural and technological parameters that provide a more complete coverage of the seed surface with biological products while simultaneously sparing the effects on biological products and seeds. The purpose of the study is to build a mathematical model of the movement of seeds in a drum-type treater with a non-stationary mode of movement.

## Material and Methods

In drum treaters mixing occurs in a rotating drum with the free fall of the components lifted by the drum wall due to friction forces arising between the wall surface and the material being mixed. The duration of mixing depends on the angle of the drum to the horizon.

In the study of such installations, as a rule, it is assumed that the movement of bulk material in the drum is similar to the movement of one of its particles, taken as a material point, and the coefficient of sliding friction is taken to be a

constant value, which corresponds to its average value along the entire path of movement along the surface.

The steady-state cycle of particle motion inside a rotating drum manifests itself in three variable states (Figure 2):

- 4-1 – relative rest;
- 1-2; 3-4 – relative movement on the drum surface;
- 2-3 – free movement.

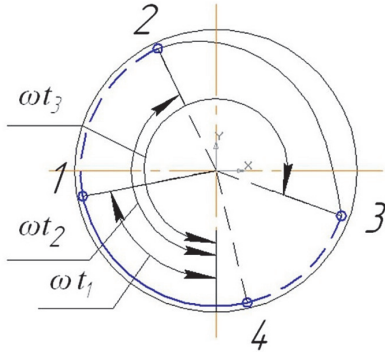


**Fig. 2. Cycle phases of the motion of a material point on the surface of the drum**

Of practical importance is the state of free movement of the particle, when there is full (over the entire surface) contact of the particle with the working mixture.

In turn, the mode of operation of the treater is characterized by the length of the trajectory of the particle flight in the phase of free movement. If at the steady-state mode of the flight paths of a particle obey the law of Gaussian distribution, then in the non-stationary mode there is no pattern in the distribution of the length of the flight of particles. Obviously, the entire working volume of the drum of the treater will be used most fully.

Let's consider the movement of a particle in the 4-1 state (Figure 2), when the grain is at rest relative to the drum wall, that is, it moves without sliding. The following forces act on the particle (material point  $M$  with mass  $m$ ) (Figure 3):

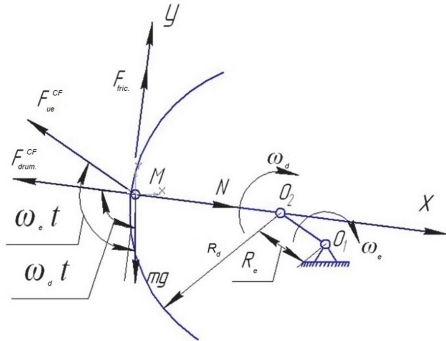


**Fig. 3. Diagram of the forces acting on the material point  $M$  in the 4-1 state**

$F_{fric}$  – is the friction force of the particle on the surface of the drum, directed tangentially to the surface in the direction of rotation of the drum:

$$F_{fric} = N \operatorname{tg} \phi, \quad (1)$$

where  $N$  is the reaction force of the support (drum wall); – is the coefficient of particle friction, which depends on its type and the surface of the drum;  $\operatorname{tg} \phi$  – is gravity, directed vertically downwards.

$F_{drump}^{CF}$  – is centripetal force of inertia of the grains, resulting from the rotational motion of the drum:

$$F_{drump}^{CF} = m \omega_d^2 R_d, \quad (2)$$

where  $\omega_d$  – is the angular velocity of rotation of the drum;  $R_d$  – is the radius of the drum.

$F_{eccentr}^{CF}$  – is the centripetal force of inertia of the particle, arising due to the rotational motion of the eccentricity:

$$F_{eccentr}^{CF} = m \omega_e^2 R_e, \quad (3)$$

where  $\omega_e$  – is the angular velocity of rotation of the eccentricity;  $R_e$  – is the magnitude (radius) of eccentricity.

Let's accept the coordinate system  $M_x$  and  $M_y$ . The axis  $M_x$  is directed to the center of the drum from a point  $M$ , the axis  $M_y$  is directed tangently to the circumference of the drum at a point  $M$  in the direction of rotation of the drum. Regarding the adopted reporting system, the sum of all forces acting on the grain  $M$  is zero, therefore the projections of these forces on the axes  $M_x$  and  $M_y$  are equal to zero:

$$\sum F M_x : N + mg \cos(\pi - \omega_d t) - F_{drump}^{CF} - F_{eccentr}^{CF} \cos(\omega_e t - (\pi - \omega_d t)) = 0, \quad (4)$$

$$\sum F M_y : F_{fric} + F_{eccentr}^{CF} \sin(\omega_e t - (\pi - \omega_d t)) - mg \sin(\pi - \omega_d t) = 0. \quad (5)$$

Let's express the force  $N$  from equation (1):

$$N = \frac{F_{mp}}{\operatorname{tg} \phi}. \quad (6)$$

Let's substitute  $N$  from expression (6) into equation (4):

$$\frac{F_{fric}}{\operatorname{tg} \phi} + mg \cos(\pi - \omega_d t) - F_{drump}^{CF} - F_{eccentr}^{CF} \cos(\omega_e t - (\pi - \omega_d t)) = 0 \quad (7)$$

$$F_{fric} = F_{drump}^{CF} + F_{eccentr}^{CF} \cos(\omega_e t - (\pi - \omega_d t)) \operatorname{tg} \phi - mg \cos(\pi - \omega_d t) \operatorname{tg} \phi \quad (8)$$

Let's analyze equation (7). For the time when  $t_4 \leq t \leq t_1$  the expression is true:

$$F_{fric}^{ult} = F_{drump}^{CF} + F_{eccentr}^{CF} \cos(\omega_e t - (\pi - \omega_d t)) \operatorname{tg} \phi - mg \cos(\pi - \omega_d t) \operatorname{tg} \phi \quad (9)$$

$$F_{fric.}^{ult.} = F_{drum}^{CF} + F_{eccentr.}^{CF} \cos(\omega_e t - (\pi - \omega_d t)) \operatorname{tg} \phi - mg \cos(\pi - \omega_d t) \operatorname{tg} \phi \quad (10)$$

where  $F_{fric.}^{ult.}$  is the ultimate friction force capable of holding the particle on the inner surface of the drum wall without sliding.

The condition when the particle moves without sliding can be written in the following form:

$$F_{fric.}^{ult.} \leq F_{fric.} \quad (11)$$

Over time, i.e. with an increase  $t$ , the component of gravity on the axis  $M_x mg \cos(\pi - \omega_d t)$  will increase due to an increase in the angle  $\omega_d t$ . This will lead to the fact that at the moment of time  $t_1$  the right side of inequality (11) decreases to a value  $F_{fric.}^{ult.}$ . Inequality (11) takes the form:

$$F_{fric.}^{ult.} = F_{drum}^{CF} + F_{eccentr.}^{CF} \cos(\omega_e t - (\pi - \omega_d t)) \operatorname{tg} \phi - mg \cos(\pi - \omega_d t) \operatorname{tg} \phi \quad (12)$$

Equation (12) characterizes the position of the particle at point 1 (Figure 2), when the grain begins to slip relative to the drum surface.

Equation (12) for the moment of time  $t_1$  takes the form:

$$F_{fric.}^{ult.} + F_{eccentr.}^{CF} \sin(\omega_e t_1 - (\pi - \omega_d t_1)) - mg \sin(\pi - \omega_d t_1) = 0 \quad (13)$$

Let's express  $F_{fric.}^{ult.}$  from equation (13):

$$F_{fric.}^{ult.} = mg \sin(\pi - \omega_d t_1) - F_{eccentr.}^{CF} \sin(\omega_e t_1 - (\pi - \omega_d t_1)) \quad (14)$$

Equating the right sides of equations (12) and (14), we obtain the equation for determining the time  $t_1$ :

$$F_{drum}^{CF} + F_{eccentr.}^{CF} \cos(\omega_e t_1 - (\pi - \omega_d t_1)) \operatorname{tg} \phi - mg \cos(\pi - \omega_d t_1) \operatorname{tg} \phi = mg \sin(\pi - \omega_d t_1) - F_{eccentr.}^{CF} \sin(\omega_e t_1 - (\pi - \omega_d t_1))$$

$$F_{drum}^{CF} + F_{eccentr.}^{CF} \cos(\omega_e t_1 - \omega_d t_1 - \pi) \operatorname{tg} \phi - mg \cos(\pi - \omega_d t_1) \operatorname{tg} \phi - mg \sin(\pi - \omega_d t_1) + F_{eccentr.}^{CF} \sin(\omega_e t_1 + \omega_d t_1 - \pi) = 0 \quad (15)$$

Using the reduction formulas, simplifying equation (15), we obtain:

$$F_{drum}^{CF} - F_{eccentr.}^{CF} \cos(\omega_e t_1 - \omega_d t_1) \operatorname{tg} \phi + mg \cos(\omega_d t_1) \operatorname{tg} \phi - mg \sin(\omega_d t_1) - F_{eccentr.}^{CF} \sin(\omega_e t_1 + \omega_d t_1) = 0 \quad (16)$$

Substituting the expressions  $F_{drum}^{CF}$  and  $F_{eccentr.}^{CF}$  from (2) and (3) into equation (16) and reducing both parts to  $m$ , we get:

$$\omega_d^2 R_d - \omega_e^2 R_e \cos(\omega_e t_1 + \omega_d t_1) \operatorname{tg} \phi + g \cos(\omega_d t_1) \operatorname{tg} \phi - g \sin(\omega_d t_1) - \omega_e^2 R_e \sin(\omega_e t_1 + \omega_d t_1) = 0 \quad (17)$$

Equation (14) allows us to determine the time  $t_1$  when the particle begins to slip against the drum surface. In turn, time al-

lows us to determine the angle  $\omega_d t$  – how much the drum turns before the particle starts to slip, and the angle  $\omega_e t$  – the position of the eccentricity at the moment the particle starts to slip.

A distinctive feature of the behaviour of a particle in the 1-2 state is (Figure 4) that the particle moves relative to the surface of the drum with negative angular acceleration .

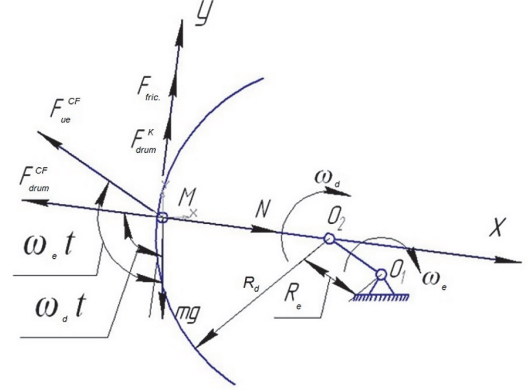


**Fig. 4. Diagram of the forces acting on the material point  $M$  in the state of 1-2**

As a result, the particle is additionally affected by one more force  $F_{drum}^{TF}$  – the tangential force of inertia of the particle relative to the drum, directed along the tangent to the circumference of the cross section of the drum in the direction of rotation of the drum. Force  $F_{drum}^{TF}$  is expressed as:

$$F_{drum}^{TF} = m \epsilon R_d \quad (18)$$

The position of the particle relative to the surface of the drum is determined by the angle  $\omega_d t$  –  $\omega t$  where  $\omega$  is the angular velocity of the grain relative to the surface of the drum,  $c^{-1}$ .

The projection of forces on the axis  $M_x$  and  $M_y$  allows defining two equations:

$$\sum F M_x = 0 : N + mg \cos(\pi - (\omega_d t - \omega t)) - F_{drum}^{CF} - F_{eccentr.}^{CF} \cos(\omega_e t - (\pi - \omega_d t)) = 0 \quad (19)$$

$$\sum F M_y = 0 : F_{fric.} + F_{drum}^{TF} + F_{eccentr.}^{CF} \sin(\omega_e t - (\pi - \omega_d t + \omega t)) - mg \sin(\pi - \omega_d t + \omega t) = 0 \quad (20)$$

The joint solution of equations (19) and (20) leads to the following equation:

$$\epsilon = \frac{d\omega}{dt} = \omega_d^2 \operatorname{tg} \phi + \frac{g}{R_d} \cos(\omega_d t - \omega t) + \frac{\omega_e^2 R_e}{R_d} \cos(\omega_e t + \omega_d t) - \frac{\omega_e^2 R_e}{R_d} \sin(\omega_e t - \omega_d t + \omega t) - \frac{g}{R_d} \sin(\omega_d t + \omega t) \quad (21)$$

Under this condition, the detachment of the particle from the surface of the drum is the equality of the reaction  $N$  zero:

$$N = 0 \quad (22)$$

The projection of forces on the axis  $M_x$  takes the for:

$$mg \sin(\omega_d t - \omega t - 90^\circ) - F_{drum}^{CF} - F_{eccentr.}^{CF} \cos(\omega_e t - \omega_d t + \omega t) = 0 \quad (23)$$

After simplifying the expression, we obtain an equation characterizing the position of the particle at time  $t_2$ , when it is detached from the drum surface:

$$\cos(\omega t_2 - \omega_d t_2) + (\omega_d - \omega)^2 R_d + \omega_e^2 R_e \cos(\omega_e t_2 - \omega_d t_2 + \omega t_2) = 0 \quad (24)$$

The absolute speed of the grain at time  $t_2$  relative to the  $O_2$  point is determined by the expression:

$$\Omega = \omega_d - \omega, \quad (25)$$

where  $\Omega$  is the absolute velocity of the particle.

The angle of inclination of the tangent to the trajectory of the particle at time  $t_2$  is determined by the angle  $\omega_d t_2$ . The position of the eccentricity is determined by the angle  $\omega_e t_2$ .

In the future, equation (24) and integration of equation (21) give a system of equations of a mathematical model of the behaviour of a particle in the state of 1-2, with which we can justify the non-stationary mode of movement of seeds within the working drum.

Let's consider the cycle of free movement of a particle (flight) when it moves independently of the surface inside a rotating drum.

We accept the coordinate system with the beginning at the point  $O_2$ . We will direct an axis  $O_2 x$  horizontally; axis  $O_2 y$  vertically, as shown in Figure 5.

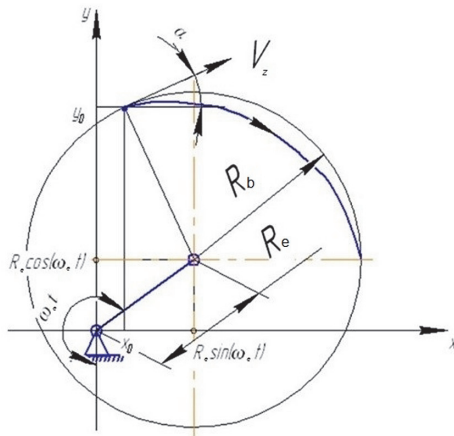


Fig. 5. Calculation scheme

The flight of a body thrown at an angle to the horizon is described as follows:

$$\begin{cases} x = x_0 + V_0 t \cos \alpha \\ y = y_0 + V_0 t \sin \alpha - \frac{gt^2}{2} \end{cases} \quad (26)$$

where  $x_0$  is the projection of the point  $M$  on the axis  $O_2 x$ .

In our case:

$$\begin{aligned} x_0 &= -R_e \cos(\omega_e t_2 - \frac{\pi}{2}) - R_d \cos(\omega_d t_2 - \omega t_2 - \frac{\pi}{2}) = \\ &= R_e \cos(\frac{\pi}{2} - \omega_e t_2) - R_d \cos(\frac{\pi}{2} - \omega_d t_2 + \omega t_2) = \\ &= -R_e \sin(\omega_e t_2) - R_d \sin(\omega_d t_2 + \omega t_2) \end{aligned} \quad (27)$$

$V_0$  is the initial particle velocity,  $V_0 = V_z$ ;  $y_0$  is the projection of the point  $M$  on the axis  $O_2 y$ . For our case:

$$\begin{aligned} y_0 &= -R_e \sin(\omega_e t_2 - \frac{\pi}{2}) + R_d \sin(\omega_d t_2 - \omega t_2 - \frac{\pi}{2}) = \\ &= -R_e \sin(\frac{\pi}{2} - \omega_e t_2) - R_d \sin(\frac{\pi}{2} - \omega_d t_2 + \omega t_2) = \\ &= -R_e \cos(\omega_e t_2) - R_d \cos(\omega_d t_2 - \omega t_2) \end{aligned} \quad (28)$$

$$\begin{cases} t - \text{is the particle flight time, for our case } t_0 = t_2 \\ x = -R_e \sin(\omega_e t_2) - R_d \sin(\omega_d t_2 + \omega t_2) + V_z(t - t_2) \cos \alpha \\ y = -R_e \cos(\omega_e t_2) - R_d \cos(\omega_d t_2 - \omega t_2) + \\ + V_z(t - t_2) \sin \alpha - \frac{g(t - t_2)^2}{2} \end{cases} \quad (29)$$

The system of equations (29) describes the motion of a particle during free flight, i.e. it determines the position (coordinates  $x$  and  $y$ ) depending on time  $t$ .

The surface of the drum in cross section is projected into a circle described by the following equation:

$$(x - x_0)^2 + (y - y_0)^2 = R^2, \quad (30)$$

where  $x_0$  is the deviation of the center of the circle along the axis  $O_2 x$ ;  $x_0 = R_e \sin(\omega_e t)$ ;  $y_0$  is the axis deviation of the center of the circle  $O_2 y$ ;  $y_0 = R_e \cos(\omega_e t)$ ;  $R$  is the radius of the drum,  $R = R_d$ .

From here:

$$(x - R_e \sin(\omega_e t))^2 + (y - R_e \cos(\omega_e t))^2 = R_d^2 \quad (31)$$

Expression (31) is an equation of a circle with the radius  $R_d$  of the drum surface, the center of which, in turn, moves around the circle with a radius  $R_e$  (eccentricity) depending on time.

The mutual solution of equation (31) and system of equations (29) gives the coordinates of point 3 ( $x_3, y_3$ ) at the time when the point of position of the particle  $M$  lies on the drum circumference, i.e. it is picked up by the surface of the drum:

$$\begin{cases} x = -R_e \sin(\omega_e t_2) - R_d \sin(\omega_d t_2 + \omega t_2) + V_z(t - t_2) \cos \alpha \\ y = -R_e \cos(\omega_e t_2) - R_d \cos(\omega_d t_2 - \omega t_2) + \\ \quad + V_z(t - t_2) \sin \alpha - \frac{g(t - t_2)^2}{2} \\ (x - R_e \sin(\omega_e t))^2 + (y - R_e \cos(\omega_e t))^2 = R_d^2 \end{cases} \quad (32)$$

Thus, the derived system of equations in an implicit form, which allows to determine the time corresponding to a particle hit the drum surface, makes it possible to determine the duration of its free flight, i.e. time when there is a full (over the entire surface) contact of the particle with the bio product.

Substantiation of the design parameters of the treater with an eccentrically fixed drum in the future should be aimed at increasing the duration and achieving the dispersion of the value of this time, which will allow improving the quality of seed treatment and reducing the constructive dimensions of the treater.

## Results and Discussion

The derived equations (17, 21, 24) and the system of equations (32) allow us to determine the required values for the study of  $t_1$  (time when the seed begins to slip relative to the drum surface),  $t_2$  (time of the seed position at the moment of detachment relative to the drum surface),  $\omega$  (angular seed slipping speed relative to the drum surface) and  $t_3$  (time of position of the seed at the moment of crossing with the drum surface).

All determined values are interdependent, so  $t_1$  allows determining  $t_2$  and  $\omega$ ;  $t_2$  and  $\omega$  allow us to determine  $t_3$ ; the difference  $t_3$  and  $t_2$  gives in turn  $\Delta t$ .  $\Delta t = t_3 - t_2$  - is the seed flight time.

To determine the optimal value of the radius of the crank we use the following method:

- Set the value of  $R_e$ ;
- Collect a series of data characterizing the ingress of seed onto the drum surface at various positions of the angle of rotation of the crank. Obviously, the full cycle will be one full cycle of the crank around its axis.

We divide the full cycle of crank rotation into 29 sections with 30 points, with step  $i$ :

$$i = \frac{\omega_e}{2\pi * 29}, [\text{s}];$$

where  $i$  is the time step corresponding to the angle of rotation of the crank at the angle of  $\frac{2\pi}{29}$ ;  $\omega_e$  - is the angular velocity of the crank,  $\text{s}^{-1}$ .

For research, we specify the angular velocity of the crank  $\omega_e = 5 \text{ s}^{-1}$ . Further, after determining the optimal radius of

the crank  $R_e$ , the angular velocity of the crank  $\omega_e$  will also be optimized.

The experiment step  $i$  is set in time, since the mathematical model includes time  $t$  as a variable. The derived equations (17, 21, 24) and the system of equations (32) are transformed in such a way as to be able to change the initial angle of rotation of the crank, i.e. in all expressions  $\omega_e t$  is replaced by  $t + i$ :  $\omega_e t = \omega_e(t + i)$ . The angle of rotation of the grain relative to the center of the drum is  $\omega_d t$ :

$$\omega_d^2 R_d \text{tg} \phi - \omega_e^2 R_e \cos(\omega_e(t_1 + i) + \omega_d t_1) \text{tg} \phi + g \cos(\omega_d t_1) \text{tg} \phi - g \sin(\omega_d t_1) - \omega_e^2 R_e \sin(\omega_e(t_1 + i) + \omega_d t_1) = 0 \quad (33)$$

$$\begin{cases} \frac{t_2^2}{2} \omega_d^2 \text{tg} \phi + \frac{g \sin(\omega_d t_2 - \omega t_2)}{R_d(\omega_d - \omega)} + \frac{\omega_e^2 R_e \sin(\omega_e(t_2 + i) + \omega_d t_2)}{R_d(\omega_e + \omega_d)} + \\ \frac{\omega_e^2 R_e \cos(\omega_e(t_2 + i) - \omega_d t_2 + \omega t_2)}{(\omega_e - \omega_d + \omega)} + \frac{g \cos(\omega_d t_2 - \omega t_2)}{R_d(\omega_d - \omega)} \\ - \frac{t_1^2}{2} \omega_d^2 \text{tg} \phi - \frac{g \sin(\omega_d t_1 - \omega t_1)}{R_d(\omega_d - \omega)} + \frac{\omega_e^2 R_e \sin(\omega_e(t_1 + i) + \omega_d t_1)}{R_d(\omega_e + \omega_d)} - \\ \frac{\omega_e^2 R_e \cos(\omega_e(t_1 + i) - \omega_d t_1 + \omega t_1)}{(\omega_e - \omega_d + \omega)} - \frac{g \cos(\omega_d t_1 - \omega t_1)}{R_d(\omega_d - \omega)} - \omega = 0 \\ g \cos(\omega t_2 - \omega_d t_2) + (\omega_d - \omega)^2 R_d + \\ + \omega_e^2 R_e \cos(\omega_e(t_2 + i) - \omega_d t_2 + \omega t_2) = 0 \end{cases} \quad (34)$$

$$\begin{cases} x = -R_e \sin(\omega_e(t_2 + i)) - R_d \sin(\omega_d t_2 + \omega t_2) + V_z(t - t_2) \cos \alpha, \\ y = -R_e \cos(\omega_e(t_2 + i)) - R_d \cos(\omega_d t_2 + \omega t_2) + \\ \quad + V_z(t - t_2) \sin \alpha - \frac{g(t - t_2)^2}{2}, \\ (x - R_e \sin(\omega_e(t + i)))^2 + (y - R_e \cos(\omega_e(t + i)))^2 = R_d^2. \end{cases} \quad (35)$$

The time step  $i$  will have the following value:

$$i = \frac{5}{2 * 3.1415 * 29} = 0.02744 \text{ s.}$$

For different values of  $t + i$  from the crank rotation cycle, we determine the value of time  $t_1$  from expression (33) in the MatCad program. We do the same to determine the moments of time  $t_2$ , the angular sliding velocities of the grain  $\omega$ , and the moments of time  $t_3$ . Next, the time of flight of the seed  $\Delta t$  is determined, corresponding to different values of the initial angle of rotation of the crank  $\omega_e(t + i)$  at the moment the seed hits the surface of the drum.

We increase the value of  $R_e$  by 0.003 m until it is possible to determine all the quantities from equation (33) and system of equations (34) and (35). This moment, when one of the equations becomes unsolvable, characterizes the behaviour of the system that goes beyond the variable states of the particle's motion cycle inside a rotating drum.

In our case, the system of equations (34) has become unsolvable when the crank radius value is  $R_e = 0.054$  m.

The optimal value of the crank radius will be determined by the following criteria:

1. Total accumulated flight time  $\Sigma\Delta t$ , s. It characterizes the total flight time of seeds falling on the drum surface with a step  $\omega_e(t + i)$  during one cycle of the crank. The higher the value  $\Sigma\Delta t$ , the more time the seeds spend in free flight and have full contact with the bio product.

2. Non-stationarity of the mode of movement of seeds is characterized by a spread of values  $\Delta t$ , i.e. interval

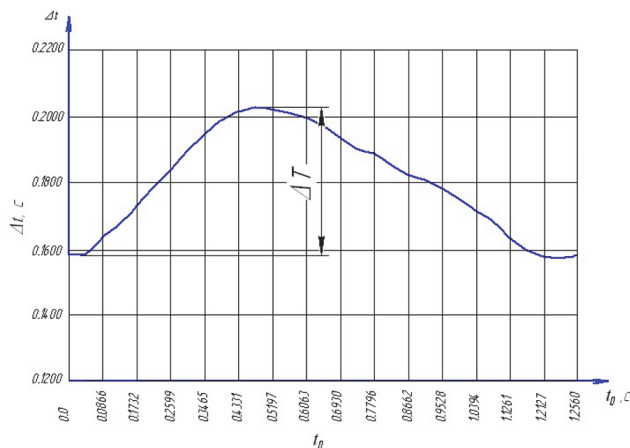


Fig. 6. The graph of dependencies  $\Delta t = f(t_0)$  at  $R_e = 0.03$  m

$\Delta T = \Delta t_{min_{max}}$  [s]. The higher the value  $\Delta T$ , the higher the area in the cross section of the drum, which is covered by seeds that are in free flight, and the higher the efficiency of the installation.

3. The radius of the crank  $R_e$ . The higher the  $R_e$ , the greater the inertial forces acting on the treater nodes, the higher the vibration, the noise and the percentage of seed damage due to the impact. It is necessary to take  $R_e$  as little as possible.

For each value of the series  $\Delta t$ , we determine  $\Sigma\Delta t$ , and  $\Delta T$  is the amplitude of the curve  $\Delta t$  (Figure 6).

According to  $\Sigma\Delta t$ , and  $\Delta T$  we construct dependency graphs  $\Delta t = f(t_0)$  for different values of  $R_e$  (Figure 7). From Figure 7 it is seen that with increasing  $R_e$  the position of the graph  $\Sigma\Delta t = f(R_e)$  rises, and the interval of the graph  $\Delta T = f(R_e)$  increases.

According to the data  $\Sigma\Delta t$  and  $\Delta T$  we construct dependency graphs  $\Sigma\Delta t = f(R_e)$  (Figure 8) and  $\Delta T = f(R_e)$  (Figure 9).

Based on the criteria above, we take  $R_e = 0.03m$  as the optimum value for the radius of the crank. From the graph of dependences  $\Sigma\Delta t = f(R_e)$ , it can be seen that a further increase in the crank radius does not lead to an increase in the total accumulated flight time of the grain. The interval (amplitude)  $\Delta t$  continues to grow with an increase in the crank radius, but the device vibration and the proportion of damaged seeds increase as well.

To determine the optimal angular velocity of the crank we use a method similar to the method of determining the size of the crank.

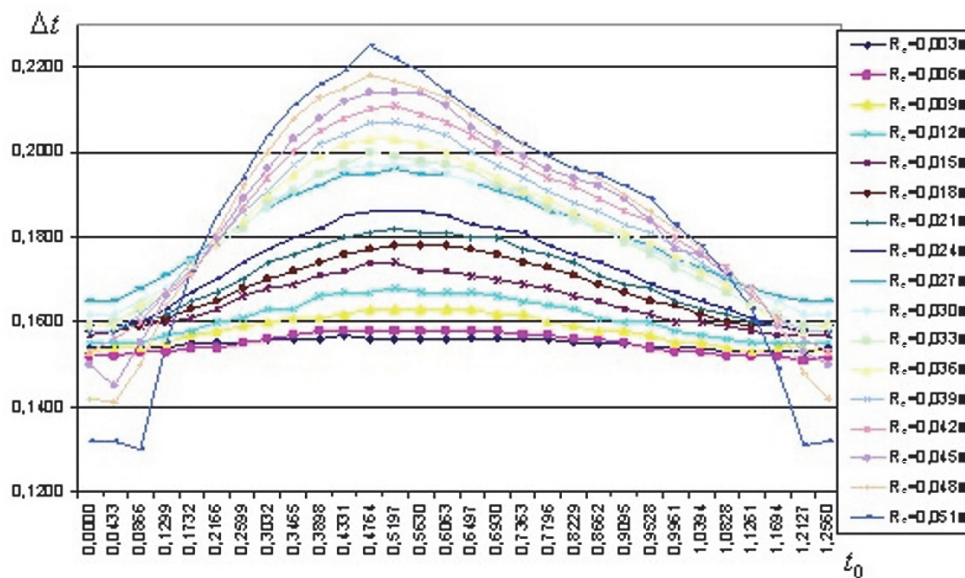
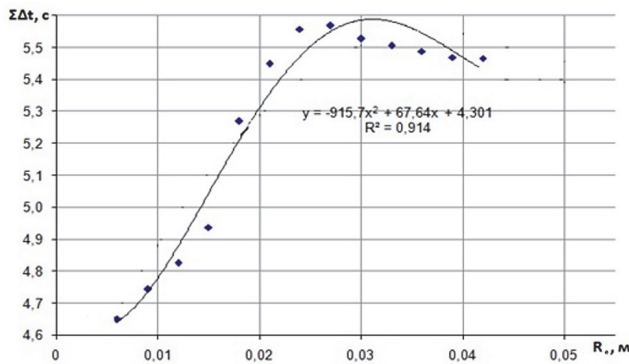
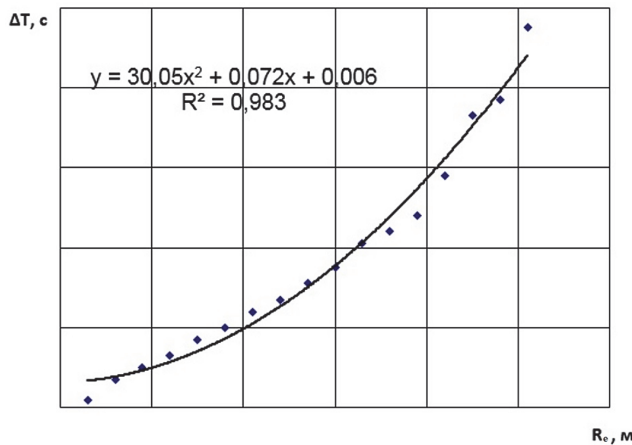


Fig. 7. Graphs of dependences of the duration of the flight of the seed  $\Delta t$  on the time corresponding to the initial angle of rotation of the eccentricity  $t_0$  at different values of the crank radius  $R_e$



**Fig. 8.** Graph of dependency of accumulated time of the seed flight  $\Sigma\Delta t$  on the radius of the crank  $R_e$



**Fig. 9.** Graph of the dependence of the descent interval  $\Delta T$  on the radius of the crank  $R_e$

We are given a series of values of  $\omega_e$ , for each of which we determine a series of values  $\Delta t$ . We investigate this series, i.e. we determine the total accumulated flight time  $\Sigma\Delta t$ , we determine the interval of values  $\Delta t$ :  $\Delta T = \Delta t_{min}^{max}$ . According to the obtained values, we construct dependency graphs  $\Sigma\Delta t = f(\omega_e)$  and  $\Delta T = f(\omega_e)$ , by which we determine the optimal value of the angular velocity of the crank  $\omega_e$ .

When setting a number of values of  $\omega_e$ , we use the results of research obtained by us experimentally. Studies have shown that the optimal value of  $\omega_e$  lies within 4 ... 8 s<sup>-1</sup>. Proceeding from this, we set a series  $\omega_e = 2; 4; 6; 8$  s<sup>-1</sup>. It also makes sense to use negative values of  $\omega_e$ , i.e. when the crank rotates opposite to the rotation of the drum. We take the series  $\omega_e = -8; -6; -4; -2; 2; 4; 6; 8$  s<sup>-1</sup>.

When determining the optimal value of  $\omega_e$ , the full cycle of crank rotation is variable for different values of  $\omega_e$ . There-

fore, for research, we take a series of  $t$  values from the interval corresponding to the full crank cycle with the minimum value of  $\omega_e$ , i.e. when  $\omega_e = 2$  s<sup>-1</sup>. Turnover time is determined from the expression:

$$t = \frac{2\pi}{\omega_e} = \frac{2\pi}{2} = \pi = 3.14 \text{ s.}$$

Obviously, for the time  $t = 3.14$  s, the number of cycles (revolutions) for the case  $\omega_e = 8$  s<sup>-1</sup> will be:

$$N = \frac{\omega_e^{(8)}}{\omega_e^{(2)}} = \frac{8}{2} = 4.$$

On this basis, for greater accuracy of calculations, we divide the time  $t = 3.14$  s not by 29, but by 40 plots and the number of points  $n = 41$ .

We define a series with a step:

$$i = \frac{t}{40} = \frac{3.14}{40} = 0.0785 \text{ s.}$$

$$t = 0; 0.0785; 0.1570; \dots; 3.14 \text{ s}$$

For each value of  $\omega_e$  we define the results of calculations  $t_1, t_2, \omega, t_3$  and  $\Delta t$  for a series of values  $t = 0; 0.0785; 0.1570; \dots; 3.14$  s. According to the obtained  $\Delta t$  data, we construct the dependence graph  $\Delta t = f(t)$  (Figure 10). It is seen that the graph is a sinusoid tilted to the left. The sine wave period is equal to the crank rotation time.

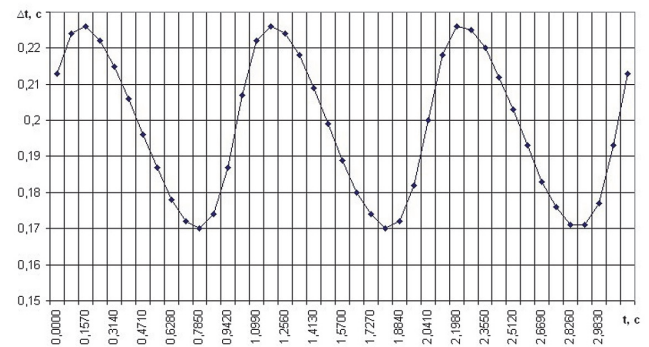


**Fig. 10.** Dependency graph of seed flight duration on time with  $\omega_e = 6$  s<sup>-1</sup>

According to the  $\Delta t$  data obtained during the calculations, we determine the total accumulated flight time  $\Sigma\Delta t$  and the interval  $\Delta T$ , using the data obtained, we construct the dependency graphs  $\Delta T = f(\omega_e)$  (Figure 11) and  $\Delta t = f(\omega_e)$  (Figure 12).

From Figure 11 it can be seen that the total accumulated flight time of the grain grows with an increase in the module



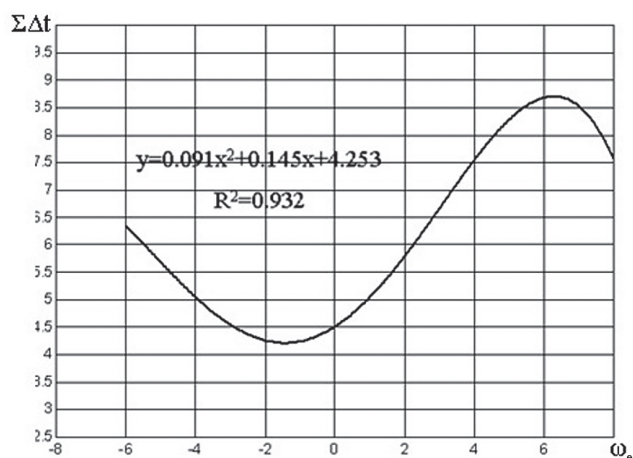


**Fig. 11.** Graph of dependency of the total accumulated time of flight of the seed  $\Sigma\Delta t$  on the angular velocity of the crank  $\omega_c$

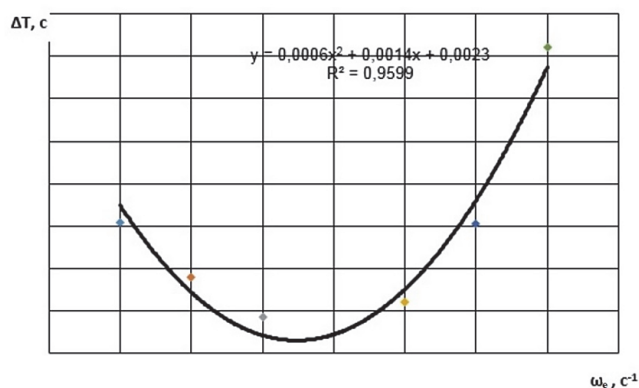


**Fig. 12.** Graph of dependency of the amplitude  $\Delta T$  on the angular velocity of the crank  $\omega_c$

of the angular velocity of rotation of the crank to  $\omega_c = 6 \text{ s}^{-1}$  and decreases with its further increase, and the growth of  $\Sigma\Delta t$  with negative values of  $\omega_c$  lags. This suggests that with the same magnitude of the module of the angular velocity of eccentricity, it is more acceptable to choose the direction of rotation of the crank, which coincides with the direction of rotation of the drum. The same explains the slope of the sinusoid – the graph of dependence  $\Sigma\Delta t = f(t)$  (Figure 10) and the change in the slope of the sinusoid when the direction of rotation of the crank is changed.

The graph of the dependence  $\Delta T = f(\omega_c)$  (Figure 12) generally repeats the behaviour of the graph of the dependence  $\Sigma\Delta t = f(\omega_c)$ . The graph  $\Delta T = f(\omega_c)$  has maximum values at angular velocity values  $\omega_c = -6 \text{ s}^{-1}$  and  $\omega_c = 6 \text{ s}^{-1}$ . It is seen

that the angular speed of rotation of the crank has optimal values at values close in magnitude to the angular velocity of rotation of the drum.

## Conclusions

The constructed mathematical model of the movement of the seed inside the eccentrically fixed drum of the seed treater promotes fuller utilization of the working volume of the drum and high-quality coating of seeds with preparations.

Based on the theoretical studies of seed movement in an eccentrically fixed drum and modelling using the Mathcad program, it has been established that the total seed flight time inside the drum increases with an increase in the radius of its crank to 0.03 m and if the direction of rotation of the crank coincides with its direction of rotation. The design and technological parameters of the drum treater are determined at which a high-quality seed coating with a preparation is achieved: crank radius  $R_c = 0.03 \text{ m}$ ; crank rotation frequency  $\omega_c = 6 \text{ s}^{-1}$ , and the direction of rotation of the eccentricity coincides with the direction of rotation of the drum.

According to the results of theoretical studies, experimental drum treaters with a capacity of 1.5; 4; 10 t/h are designed and tested. The quality of the seed coating with the product meets agro-technical requirements the coverage ratio was more than 98%. It was determined that in order to ensure a productivity of 4 t/h, the treater should have the following design parameters: drum diameter – 0.5 m; length – 1.5 m, the angle of the drum should be made with the possibility of change in the range of 6 ... 10°. The use of a treater with an eccentrically fixed drum with a capacity of 4 t per hour during the pre-sowing treatment of seeds allowed increasing the yield of spring wheat by 12.7%.

## References

- Annis, P. C. (2016). Chemicals for grain production and protection. *Encyclopaedia of Food Grains*, 4, 99-104.
- Cessna, A. J., & Westcott, N. D. (2018). Fate of pesticides applied to cereals under field conditions. In: *Pesticide Interactions in Crop Production: Beneficial and Deleterious Effects*, 59-85.
- Gurav, R., Tang, J., & Jadhav, J. (2017). Novel chitinase producer *Bacillus pumilus* RST25 isolated from the shellfish processing industry revealed antifungal potential against phytopathogens. *International Biodeterioration and Biodegradation*, 125, 228-234.
- Hozzein, W. N., Abuelsoud, W., Wadaan, M. A. M., Shuikan, A. M., Selim, S., Al Jaouni, S., & Abdelgawad, H. (2019). Exploring the potential of actinomycetes in improving soil fertility and grain quality of economically important cereals. *Science of the Total Environment*, 651, 2787-2798.
- Ivantsova, E., Semenenko, S., Matveeva, A., Denisov, A., &

- Kolmukidi, S.** (2015). The impact of pesticides on soil microorganisms. *International Multidisciplinary Scientific Geo Conference Surveying Geology and Mining Ecology Management, SGEM, 1*(5), 913-920.
- Kadege, E., & Lyimo, H. J. F.** (2015). Prevalence and control of wheat (*Triticum aestivum* L.) seed borne fungi in farmer-saved seeds. *Archives of Phytopathology and Plant Protection, 48*(7), 601-610.
- Kamaletdinov, R. R., Hasanov, J. R., Galljamov, F. N., & Bajguskarov, M. H.** (2009a). Reduction of seed damage during dressing. Scientific support of sustainable functioning and development of the agro-industrial complex. In: *Materials of the All-Russian Scientific-practical Conference with International Participation in the Framework of the XIX International Specialized Exhibition "AgroComplex-2009. Part I.* Bashkir State Agrarian University, Ufa.
- Kamaletdinov, R. R., Hasanov, J. R., Hajrullin, R. M., & Bajguskarov, M. H.** (2009b). *Patent for utility model # 87600. Device for presowing treatment of seeds.* Registered in the State Register of Utility Models of the Russian Federation.
- Kamaletdinov, R. R., Hasanov, J. R., Hajrullin, R. M., Siraev, R. H., & Minina, T. S.** (2007). Features of machines for processing crops with biological products. *Mechanization and Electrification of Agriculture, 6*, 2-3.
- Kosulnikov, Y. V., & Laktionov, Y. V.** (2018). Factors which influence toxicity of legume seed disinfectants towards biologicals based on symbiotic nitrogen fixers. *Sel'skokhozyaistvennaya Biologiya, 53*(5), 1037-1044.
- Li, Y., An, J., Dang, Z., Lv, H., Pan, W., & Gao, Z.** (2018). Treating wheat seeds with neonicotinoid insecticides does not harm the rhizosphere microbial community. *PLoS ONE, 13*(12), e0205200.
- Lopez-Reyes, J. G., Gilardi, G., Garibaldi, A., & Gullino, M. L.** (2016). *In vivo* evaluation of essential oils and biocontrol agents combined with heat treatments on basil cv Genovese Gigante seeds against *Fusarium oxysporum* f. sp. *basilici*. *Phytoparasitica, 44*(1), 35-45.
- Moharam, M. H., Stephan, D., & Koch, E.** (2018). Evaluation of plant-derived preparations and microorganisms as seed treatments for control of covered kernel smut of sorghum (*Sporisorium sorghi*). *Journal of Plant Diseases and Protection, 125*(2), 159-166.
- Najar, A., Ben Fek, I., Ben Ghanem, H., Kumari, S. G., & Varsani, A.** (2017). Barley yellow dwarf virus – PAV management using seed-treatment with the insecticide imidacloprid. *Arab Journal of Plant Protection, 35*(3), 178-184.
- Nasu, É. D. G. C., Amora, D. X., Monteiro, T. S. A., Alves, P. S., de Podestá, G. S., Ferreira, F. C., & de Freitas, L. G.** (2018). Pochonia chlamydsoporia applied via seed treatment for nematode control in two soil types (Article). *Crop Protection, 114*, 106-112.
- Oral, Z., Mereke, A., Kazhybek, A., Sabina, S., & Zulfia, T.** (2018). Creation of new analogues of natural phytohormons for increasing the yield of agricultural crops. *International Journal of Engineering and Technology (UAE), 7*(3), 59-61.
- Reznichenko, M. J.** (1964). *Cylindrical drums of grain cleaning machines.* Mechanical Engineering, Moscow.
- Rudelt, J., Klink, H., & Verreet, J.-A.** (2017). Einfluss der Zusammensetzung der Beizlösung auf die Staubentwicklung an Getreidesaatgut. *Journal für Kulturpflanzen, 69*, 303-308.
- Zaller, J. G., König, N., Tiefenbacher, A., Muraoka, Y., Querner, P., Ratzenböck, A., Bonkowski, M., & Koller, R.** (2016). Pesticide seed dressings can affect the activity of various soil organisms and reduce decomposition of plant material. *BMC Ecology, 16*(1), 37.
- Zegeye, W., Dejene, M., & Ayalew, D.** (2017). Management of loose smut (*Ustilago nuda*) of barley (*Hordeum vulgare*) through seed dressing and coating materials on barley in Western Amhara Region, Ethiopia. *Feed Science and Technology, 45*(1), 56-71.